Mode Shape-Based Damage Localization in Steel Plates Using a Detection Index Based on 2D Wavelet Analysis

Mohtasham Khanahmadi [1] ; **Majid Gholhaki [2*]** ; **Omid Rezaifar [2]** ; **Adel Younesi [3]**

1. M.Sc. of Structural Engineering, Faculty of Civil Engineering, Semnan University, Semnan, Iran
2. Professor, Faculty of Civil Engineering, Semnan University, Semnan, Iran
3. Ph.D. of Structural Engineering, Faculty of Civil Engineering, Semnan University, Semnan, Iran
Corresponding author: *mgholhaki@semnan.ac.ir*

ARTICLE INFO

ABSTRACT

Structures are subjected to a variety of environmental and loading conditions over time, and minor damage to structural elements may occur. By timely identifying damage and repairing damaged locations, it is possible to prevent the spread and development of damage to other elements and, as a result, the overall destruction of the structure. This article discusses the identification and determination of the location of damage in steel plates based on the use of the primary and secondary shapes of vibration modes and the analytical method of two-dimensional wavelet analysis. Modelling and frequency analysis of the plate were performed in ABAQUS software, and the primary and secondary mode shapes were extracted. To determine the location of the damage, a damage detection index (DDI) was proposed based on the angle between the primary and secondary mode shape vectors and the diagonal detail coefficients obtained from the wavelet analysis of the primary and secondary mode shapes. The results showed that by using this index, damage can be identified by identifying peaks resulting from irregularities and disturbances. Also, the DDI value of the damage was dependent on the severity of damage occurring in a damaged situation, and the height of the disorder peaks increased with increased damage only at that damage position.

1. Introduction

Some structural elements may sustain local damage over time, which may be intensified by factors like earthquakes, explosions, improper excavation, etc. and result in serious problems for the overall health of the structure. The spread of the damage to other

elements can be stopped by locating the damaged element and fixing or replacing it.

Structural health monitoring (SHM) attempts to address this problem at four levels, which are as follows [1]: (1) diagnosis of damage, (2) identification of damage locations, (3) determining the severity of damage, and (4) calculating the remaining life of the damaged structure. The present research focuses on the first two levels.

Steel plate shear wall (SPSW) is a lateral-resisting structural system which has recently become enormously popular, thanks to its application in the construction industry due to its high stiffness and resistance, high energy absorption, cost-effectiveness, and ease of implementation. Some of the more prominent advantages of SPSW include: (1) Compared to concrete shear walls, SPSWs are exposed to less earthquake load due to their lower weight; (2) Using welded or bolted connections speeds up the installation process and reduces the construction cost, in addition to the fact that there is no need for form working during the construction process; SPSWs require less space than do their equivalent reinforced concrete walls; In tall buildings, if reinforced concrete shear wall is used, wall thickness increases in the lower floors and a larger area of the floor plan is occupied; and (4) SPSW is a suitable alternative in cold regions where it is not economical to build concrete structures at very low temperatures.

Given the above benefits and the increasing use of steel plates in the construction industry, it is important to identify damage to the steel plate element.

Dynamic data (acceleration and displacement) and modal properties (natural frequencies, modal shapes, and modal damping) depend on the physical characteristics of the structure (mass, stiffness, and damping); Therefore, the occurrence of damage brings about changes in the dynamic and modal properties of the structure [2,3]. Accordingly, damage detection methods address changes in frequencies [4,5], mode shape [6,7], mode shape curvature [8–12], modal strain energy [13], Lamb Wave [14] and frequency response functions (FRFs) [15,16]. In this area, examples include the use of artificial neural networks [17,18], genetic algorithms [19,20], and fuzzy logic [21,22]. Another method of damage detection is wavelet transform (WT), which is a powerful tool for signal processing [23,24]. Due to its capacity to localize signals in both time and frequency domains, WT allows obtaining more information from analyzed signals [25]. Newland [26] proposed the concepts of WT in relation to the analysis of vibration responses. Although the author did not specifically employ WT to identify structural damage, the introduction of this method in civil, mechanical, and aerospace engineering laid the groundwork for subsequent structural health studies. Masuda et al. [27] used WT to analyze time history responses of a single-degree-of-freedom system by defining damage as a reduction in stiffness; the authors observed that WT could determine damage time even for noisy signals. Wang and Deng [28] designed a method for structural damage detection based on WT analysis of static responses. Assuming that structural damage disrupts the response of the structure, they showed that although these disruptions are not reflected in data related to the overall response, they are often identifiable by wavelet components. Hou et

al. [29] analyzed wavelet data of the San Fernando earthquake to identify damage. The results indicated that the location of peaks in the WT details corresponded to the occurrence time of damage. Using wavelet transform, Douka et al. [30] identified cracks in bending plates. They studied "an all-over part-through crack parallel to one edge of the plate" and analyzed the vibration modes of the plate by using continuous wavelet transform (CWT). Next, they detected the crack location using the proposed method and considering the sudden change in displacement response. Ovanesova and Suarz [31] used wavelet transform to identify the location of cracks in beams and frames under different loading conditions. Using trial and error, they found the biorthogonal wavelet as the most effective wavelet for damage identification. Loutridis et al. [32] analyzed the vibration mode of double-cracked beams using CWT and observed that the WT coefficients indicate high values at the crack locations. Chang and Chen [33] applied a similar method to a cantilever beam. They first achieved the mode shapes of free vibration and natural frequencies of cracked beams. Next, the mode shapes were analyzed using WT to determine the position of the cracks. The results illustrated that larger peak values could be obtained when the crack position is near the clamped end, whereas higher scales are needed to identify the crack when it is positioned near the free end. Using harmonic class loading and wavelet analysis, Khatam et al. [34] aimed at identifying damage in beams. They considered the harmonic displacement response of beams as an input signal function for WT and effectively located the damage. Fan and Qiao [35] proposed a method to locate damage based on the two-dimensional Gaussian

wavelet transform in bending plates; they succeeded in correctly identifying the damage location and determining its approximate shape. Gökdağ and Kopmaz [36] used a combination of discrete and continuous wavelet transforms to discover damage in beams. In their proposed method, the secondary mode shape was considered as a combination of the primary mode shape plus factors such as measurement error and local damage. Therefore, a suitable approximation function that indicates the undamaged mode of the structure could be extracted using discrete wavelet transform (DWT). Also, the authors concluded, the difference between the continuous wavelet coefficients of the damaged mode and the approximate function corresponding to the undamaged mode of the structure can be a suitable indicator for estimating damage. Using DWT, Katunin [37] investigated multiple cracks on the modal responses of a beam made of polymeric laminate. The results indicated that detail coefficients provide useful information to discover the position of cracks; meanwhile, it is necessary to remove noise from the coefficients in order to do a correct identification. Wavelet transform is an effective tool for identifying multiple crack positions in one-dimensional structures. Zhong and Oyadiji [38] used stationary wavelet transform (SWT) and modal data to detect cracks in simply supported beams. SWT is a redundant transform that doubles the number of input samples, provides more accurate estimates of variances, and facilitates recognizing important features in a signal. The authors argued that the position of the damage could be discovered by analyzing the stationary wavelet of mode shape data. Bagheri and Kourehli [39] used WT to identify the

position of damages in earthquake-induced structures. They intended to determine the damage time in structures such as concrete shear walls. To this end, they investigated DWT in relation to the velocity and displacement responses of the target structures. The peak values of responses in wavelet detail coefficients were associated with the time when the damage occurred. Using two-dimensional directional Gaussian wavelets and laser scanned operating deflection shapes, Xu et al. [40] successfully detected damage in some plates. Lee et al. [41] used continuous relative wavelet entropy method to identify damage in truss bridge structures. They noted that the proposed method could locate the damage in these structures and, consequently, it could be used as an effective and efficient method of damage detection. Li and Hao [42] dealt with substructure damage identification based on wavelet-domain response reconstruction and considering damage as stiffness reduction in a 2D frame structure. Accordingly, they detected damage sites by accurately estimating the extent of the damage. Using non-separable quincunx wavelets under the influence of different energy impacts, Katunin [43] analyzed the damaged mode shapes of composite structures and showed that these wavelets help accurately localize damaged sites and prevent the boundary effect. Patel et al. [44] used WT to detect damages in reinforced concrete buildings. Having analyzed wavelets of the vibration signals that had been recorded at each floor for different masses, they found a direct relationship between wavelet coefficients and changes in the physical properties of the structure. Rahami et al. [45] used the concept of entropy in wavelet packet transform to detect damages in fixed offshore platforms.

They concluded that the rate of change in damage-sensitive components, even in the case of low-intensity damages, significantly depends on the platform. Ashory et al. [46] employed a combination of wavelet transform and "finite element model updating" to detect damage in multilayer composite laminates. They used WT to identify the damage parameters; then, they specified these parameters via optimizing an error function obtained by the genetic algorithm. Analyzing 2D wavelet of modal frequency surface (MFS), Yang and Oyadiji [47] proposed a new method for identifying delamination in multilayer composite laminates. They found that reducing the local stiffness of the layers causes a disruption in the MFS, and calculating MFS wavelet coefficient helps determine the location and shape of damage in these laminates. Using wavelet coefficient differences as well as multiresolution analysis and considering mode shapes, Zhao et al. [48] aimed at detecting damage to reinforced concrete beams and introduced a damage detection index (DDI) to identify the damaged position. Using experimental modal data, Younesi et al. [49–51] addressed the detection of debonding damage in concrete-filled tube columns. They simulated this type of damage by a thin layer of polystyrene in one of the sides of the column between the concrete core and the steel wall; besides, by using CWT of the mode shape, they could identify the debonding position of the concrete core and the steel wall. Wang et al. [52] introduced a novel damage index based on "wavelet based residual force vector" to discover damage in a tunnel structure. They developed a numerical finite element model for an underground tunnel exposed to different types of damages. The results

supported the effectiveness and efficiency of the proposed index with regard to damage detection. Using 2D DWT of steel plate mode shapes, Khanahmadi et al. [53] compared the wavelet coefficients of undamaged and damaged conditions of the first eight mode shapes. They noted that perturbations in the wavelet coefficients of the damaged states were more significant than those of undamaged states in different situations. Furthermore, the authors could accurately find the location of damages in all studied modes. They also reported that analyzing the wavelet of primary mode shapes, compared to those of higher mode shapes, leads to detecting the position of damages at a more appropriate level of wavelet coefficients. In another studies, these researchers used wavelet transform to detect damages in 3D panel and laminated composite plates; they could identify locations with different damage severities [54,55]. Yet, in another study, they comparatively dealt with damage detection in steel beams using continuous and discrete wavelet transforms. They suggested that both types of wavelet transforms help identify the position of damages with high accuracy through analyzing static and dynamic responses [56–60]. Proposing WT-based methods to identify damage in prestressed concrete slabs and RC beams, Jahangir et al. [61,62] could correctly identify the damage positions. Also, Khanahmadi et al. [63,64] proposed detection methods based on CWT and DWT to detect debonding damage in CFST composite columns, which showed the efficiency of these methods in identifying the separation areas. In [65], based on the use of CWT, the primary and secondary forms of vibration modes in beams were compared. The damage position is given by the difference between the shapes of the primary mode and the secondary mode, as shown in the diagram of the primary and secondary wavelet coefficients.

In the present study, we investigated damage identification in thin-walled steel plates. To this end, we first modeled the steel plates and subjected them to frequency analysis in ABAQUS software; subsequently, we extracted modal information, including natural frequencies and mode shapes of undamaged and damaged states. Then, we attempted to identify various damaged positions by introducing a damage detection index (DDI) based on the wavelet transform and the mode shape data collected from undamaged and damaged states.

2. Wavelet transform (WT)

Wavelet transform is one of the powerful methods of signal processing that does not involve fixed-resolution problems, unlike other similar methods (e.g., Fourier transform (FT) and short-time Fourier transform (STFT)). In fact, WT is a set of basic functions that change for each frequency resolution, and frequency components are obtained at different resolutions [66,67]. There are two kinds of wavelet transform: continuous wavelet transform (CWT) and discrete wavelet transform (DWT), which are discussed below.

2.1. Continuous wavelet transform

The CWT of the $x(t)$ signal in the range $-\infty$ to ∞ is defined using Equation (1) [30,68]:

$$\text{CWT}_{a,b}^{\psi(t),x(t)} = \int_{-\infty}^{\infty} x(t)\psi_{a,b}^{*}(t)\,dt \qquad (1)$$

where

$$\psi_{b,a}(t) = \frac{1}{\sqrt{|a|}} \psi\left(\frac{t-b}{a}\right) \qquad (2)$$

In Equation (2), a and b represent the scale and transition parameters, respectively. ψ^* denotes the complex conjugate of the mother wavelet function ψ. The mother wavelet function is defined along with the scale and transfer parameters in wavelet analysis. This feature allows multiple analysis of non-static signals; thus, picking small and large scales enables WT to select small and large intervals, respectively, on the signal for analysis.

The wavelet function must satisfy the following three conditions:

The integral of the wavelet function must be zero [69], i.e.:

$$\int_{-\infty}^{\infty} \psi(t)\,dt = 0 \qquad (3)$$

Its energy must be limited [69], i.e.:

$$\int_{-\infty}^{\infty} |\psi(t)|^2 \, dt < +\infty \qquad (4)$$

It must be the case in Equation (5) [69,70]:

$$\int_{-\infty}^{\infty} \omega^{-1} |\Psi(\omega)|^2 \, d\omega < +\infty \qquad (5)$$

Where Ψ is the Fourier transform of ψ and ω expresses frequency. Equation (3) suggests that the function is oscillating, and Equation (4) indicates that the maximum energy in the wavelet function is not unlimited for a short time interval [69].

2.2. Discrete wavelet transform

In signal processing through DWT, discretization is performed for the parameters of scale (a) and transfer (b) in Equation (2). This process is optimized if it is carried out according to Equation (6).

$$a = 2^j, \; b = 2^j k \quad j,k \in Z \qquad (6)$$

By placing the above Equation in (2), the wavelet function $\psi_{b,a}$ can be expressed as follows:

$$\psi_{j,k}(t) = 2^{-j/2} \psi\left(2^{-j}t - k\right) \qquad (7)$$

In this case, the details and approximations of step j can be calculated using Equations (8) and (9), respectively [39]:

$$D_j(t) = \sum_{k \in Z} cD_j(k)\psi_{j,k}(t) \qquad (8)$$

$$A_j(t) = \sum_{k \in Z} cA_j(k)\phi_{j,k}(t) \qquad (9)$$

Where Z is a set of positive integers; cD_j and cA_j denote the approximation and detail coefficients of step j, which are determined based on Equations (10) and (11), respectively.

$$cD_j(k) = \int_{-\infty}^{\infty} S(t)\psi_{j,k}(t)\,dt \qquad (10)$$

$$cA_j(k) = \int_{-\infty}^{\infty} S(t)\phi_{j,k}(t)\,dt \qquad (11)$$

In Equations (9) and (11), ϕ is a scale function. Finally, the signal S(t) can be expressed using Equation (12):

$$S(t) = A_J(t) + \sum_{j \le J} D_j(t) \qquad (12)$$

Equations (10) and (11) present the DWT in relation to the details and approximations of the S(t) signal, respectively. It should be noted that wavelet transforms could be generalized in a two-dimensional manner. For example, the CWT of a two-dimensional signal $f(x,y)$ can be defined using Equation (13) as follows [71].

Similarly, by discretizing the scale parameter (a) and the transfer parameters b_1 and b_2,

one can reconstruct the 2D signal $S_0(n_1, n_2)$ using Equation (14) [72]:

$$2DCWT_{a,b_1,b_2}^{\psi,f} = \frac{1}{\sqrt{a \times a}} \int_{-\infty}^{\infty} \int_{-\infty}^{\infty} f(x,y) \psi^* \left(\frac{x-b_1}{a}, \frac{y-b_2}{a} \right) dxdy \tag{13}$$

$$S_0(n_1, n_2) = \overbrace{S_j(n_1, n_2)}^{cA} + \overbrace{\sum_{j \leq J} W_j^1(n_1, n_2)}^{cV} + \overbrace{\sum_{j \leq J} W_j^2(n_1, n_2)}^{cH} + \overbrace{\sum_{j \leq J} W_j^3(n_1, n_2)}^{cD} \tag{14}$$

Where cA is the coefficient of approximation and the coefficients cV, cH, and cD are related to horizontal, vertical, and diagonal details, respectively.

3. Finite element model of thin-walled steel plate

In the ABAQUS software, we modeled a thin-walled steel plate with dimensions of 600×800 mm and 2 mm thickness. The mechanical properties of this plate were: Poisson ratio of 0.3, specific gravity of 7.850 kg/m^3, and elastic modulus of 2×10^5 MPa. The plate was studied in undamaged states and damaged scenarios D1, D2, and D3 (Table 1), and its frequency analysis within 25 mm mesh dimensions.

Damages (50×50 mm) in all scenarios were applied to the elastic modulus as a reduction in stiffness. Fig. 1 shows a graphical representation of the location of damages.

Table 1. Characteristics of local damages in the steel plate.

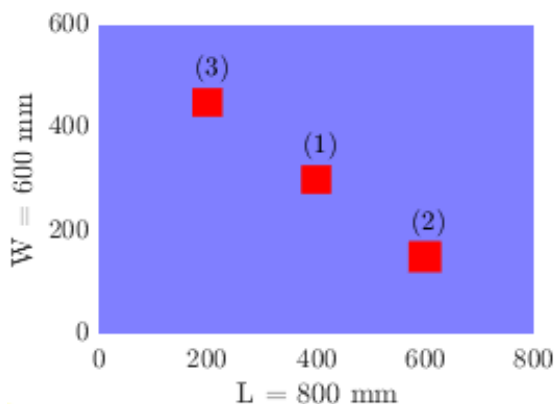| Damage			Damage Range (mm)		Damage Location		Damage Severity (%)
States	Number	Location	x	y	x/L (L = 80 cm)	y/W (W = 60 cm)	
D1	1	1	375-425	275-325	0.50	0.50	10, 20 & 30
D2	1	2	575-625	125-175	0.75	0.25	10, 20 & 30
D3	2	2	575-625	125-175	0.75	0.25	10, 20 & 30
		3	175-225	425-475	0.25	0.75	25

Fig. 1. Graphic display of damage locations of 1, 2 and 3 in the steel plate under abutment-free conditions.

4. Damage detection problem

Damage gives rise to changes in the static and dynamic responses of structures. These changes are due to alterations in the intrinsic matrices of the structure, including mass, stiffness, and damping. Accordingly, the problem of damage detection can be tackled based on changes in structural responses. In the following, these changes in natural frequencies and mode shapes are examined.

4.1. Analysis of frequency changes

Considering structural dynamics, one can express the Equation of free vibration of a structural system with n degrees of freedom without damping through Equation (15):

$$[M]\{\ddot{X}\}+[K]\{X\}=\{0\} \tag{15}$$

Where [K] and [M] matrices represent stiffness and mass, respectively. In this case, natural frequencies could be calculated by solving the characteristic Equation (16):

$$\det\left([K]-\omega^2[M]\right)=0 \tag{16}$$

Therefore, due to the direct relationship of the stiffness matrix to the elastic modulus, we expect that due to the occurrence of damage, there will be a difference in frequency values between the undamaged and damaged states. Table 2 provides the values of natural frequencies of the first four mode shapes in undamaged and damaged states. The difference in the values of the frequencies is due to a damage in the steel plate; thus, as the damage becomes more severe, the frequency difference between the undamaged and damaged states increases.

4.2. Examining changes in mode shapes

If the primary (undamaged) and secondary (damaged) mode shapes perfectly match, there is no damage in the structure and, in this case, the angle between the mode shapes will be zero. Otherwise, in the absence of this compatibility, the zero-degree angle between the vectors of corresponding mode shapes indicates that there is no damage in the structure. Conversely, one may suggest, non-zero angles confirm the occurrence of damage in the structure.

We used the concept of inner vector multiplication in order to calculate the angle between mode shape vectors. If ϕ_i^u and ϕ_i^d respectively denote the shapes of the undamaged and damaged states of the ith mode, the angle between them is determined (in units of degrees) using Equation (17) [54]:

$$\theta_i^{u,d}=\text{acosd}\left(\frac{\left(\phi_i^u\right)^T\phi_i^d}{\sqrt{\left(\phi_i^u\right)^T\phi_i^u}\sqrt{\left(\phi_i^d\right)^T\phi_i^d}}\right) \tag{17}$$

It should be noted that the square of cosine of the angle between the mode shapes is defined as the modal assurance criterion (MAC) and is always a value between zero and 1. Values less than 1 mean that the mode shape does not fully match, hence a damage in the structure. The MAC between the two shape modes of ϕ_i^u and ϕ_i^d could be determined using Equation (18) [73–76]:

$$\text{MAC}_i^{u,d}=\frac{\left(\left(\phi_i^u\right)^T\phi_i^d\right)^2}{\left(\left(\phi_i^u\right)^T\phi_i^u\right)\left(\left(\phi_i^d\right)^T\phi_i^d\right)} \tag{18}$$

Fig. 2 shows the first four mode shapes of an undamaged steel plate, and Table 3 presents the angle between the damaged mode shapes and their corresponding undamaged mode shapes. In all cases, the angle between the undamaged and damaged mode shapes is non-zero and the plate is evidently damaged.
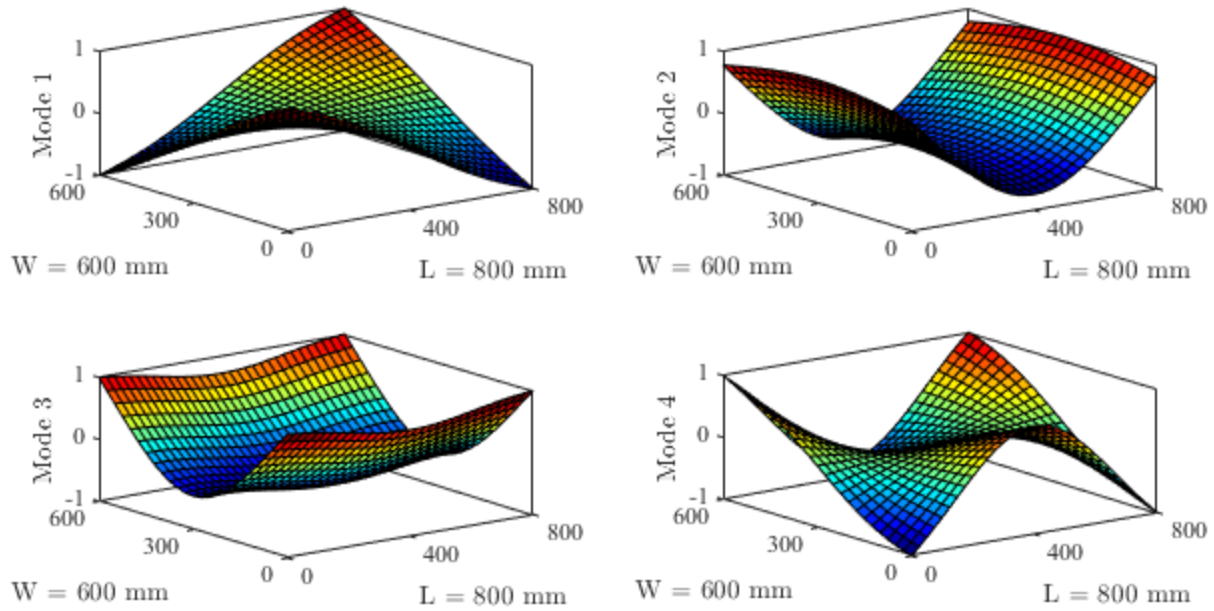
Fig. 2. Mode shapes of the undamaged steel plate.

Table 2. Natural frequencies of undamaged and damaged states of the steel plate (Hz).

Mode	PL-Un.	PL-D1 (Damage Severity (%) in Location 1)			PL-D2 (Damage Severity (%) in location 2)			PL-D3 (Damage Severity (%) in Location 3)		
		10	20	30	10	20	30	10	20	30
1	13.608	13.603	13.597	13.591	13.605	13.601	13.597	13.595	13.591	13.587
2	16.225	16.216	16.205	16.193	16.222	16.218	16.215	16.213	16.210	16.206
3	30.181	30.159	30.135	30.107	30.175	30.168	30.160	30.158	30.151	30.144
4	32.248	32.247	32.246	32.245	32.239	32.230	32.221	32.217	32.208	32.199

Table 3. Angle between damaged and undamaged mode shapes (degrees).

Mode	D1-Damage Severity in Location 1			D2-Damage Severity in Location 2			D3-Damage Severity in Location 3		
	10 %	20 %	30 %	10 %	20 %	30 %	10 %	20 %	30 %
	$\theta(U, D1)$			$\theta(U, D2)$			$\theta(U, D3)$		
1	0.0086	179.98	179.97	179.98	179.96	179.93	0.0550	0.0639	0.0803
2	0.0194	0.0427	0.0711	0.0230	0.0482	0.0764	0.0632	0.0738	0.0929
3	0.0496	0.1068	0.1738	0.0386	0.0828	0.1341	0.0891	0.0863	0.1085
4	0.0005	0.0011	0.0018	179.95	179.89	179.83	0.1621	0.1994	179.75

The concept of the angle between mode shapes is illustrated in Fig. 3. As an example, the angle between undamaged and damaged mode shapes (D1) in the first mode shows a

damage severity of 30%, equal to 179.97 degrees. It can be seen that the displacements of the nodes toward the normal vector to the plane in the damaged and undamaged states are in opposite directions.
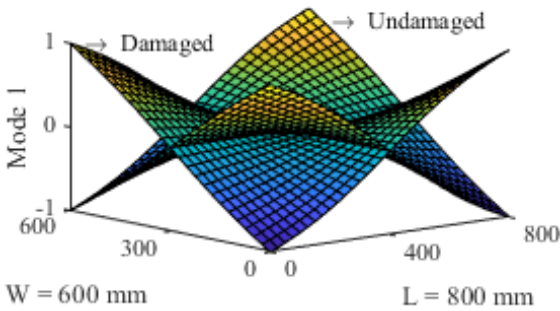

Fig. 3. The concept of angle between undamaged and damaged mode shapes (D1) in the first mode with a damage severity of 30 %.

5. Wavelet transform algorithm for detection of damage location

One of the most important features of wavelet transform, which has made it attractive for research on SHM, is the ability to spot discontinuities or sudden local changes in signals. Assuming damaged and undamaged shapes of the ith mode of the steel plate as 2D spatial signals, one can present the wavelet transform algorithm for damage detection based on the angle between the vector shapes of the ith mode as follows:

Step 1: Load damaged and undamaged shapes of ith mode to the MATLAB environment
Ui = xlsread('undamaged_mode_shape_i.xlsx');
Di = xlsread ('damaged_mode_shape_i.xlsx');
Step 2: Interpolate damaged and undamaged shapes of the ith mode
% Interpolation
Uij = interp2 (Ui, 2); Dij = interp2 (Di, 2);
Step 3: Analyze damaged and undamaged shapes of the ith mode

```
wname = 'sym4';
[cAUi, cHUi, cVUi, cDUi] = dwt2(Uij, wname);
[cADi, cHDi, cVDi, cDDi] = dwt2(Dij, wname);
```
Step 4: Calculate DDI of the ith mode
Theta_i = acosd (dot (Ui, Di) / (norm (Ui)*norm (Di));
 if floor (Theta_i) == 0
DDIi = abs (cDUi – cDDi);
elseif ceil (Theta_i) == 180
DDIi = abs (cDUi + cDDi);
end
end
Step 5: Detect damages in the ith mode
[m, n] = size(cDUi);
[x, y] = meshgrid (n, m);
surf (x, y, DDIi) % Damage detection

Investigations were performed using the analytical wavelet functions of the Daubechies, Coiflets, Symlets families. In this context, the wavelet Symlet 4 (sym4) function has been introduced as one of the most effective tools for damage detection. The results of damage detection performed on the first to fourth modes of damages (D1, D2, and D3) are respectively shown in Fig. 4 to 6 under damage severities of 10%, 20%, and 30% in the damaged locations.

It was found that the proposed WT-based algorithm can pinpoint damaged areas in all studied modes. Specifically, it was noted that with increasing damage severity, the sensitivity of DDI is heightened in fixed spatial coordinates (located in the damaged area). Besides, the results of damage detection in the damaged mode of D3 suggested that the sensitivity of the DDI of each damaged position is independent of each other, such that a damage in one area can affect only the DDI of that site.
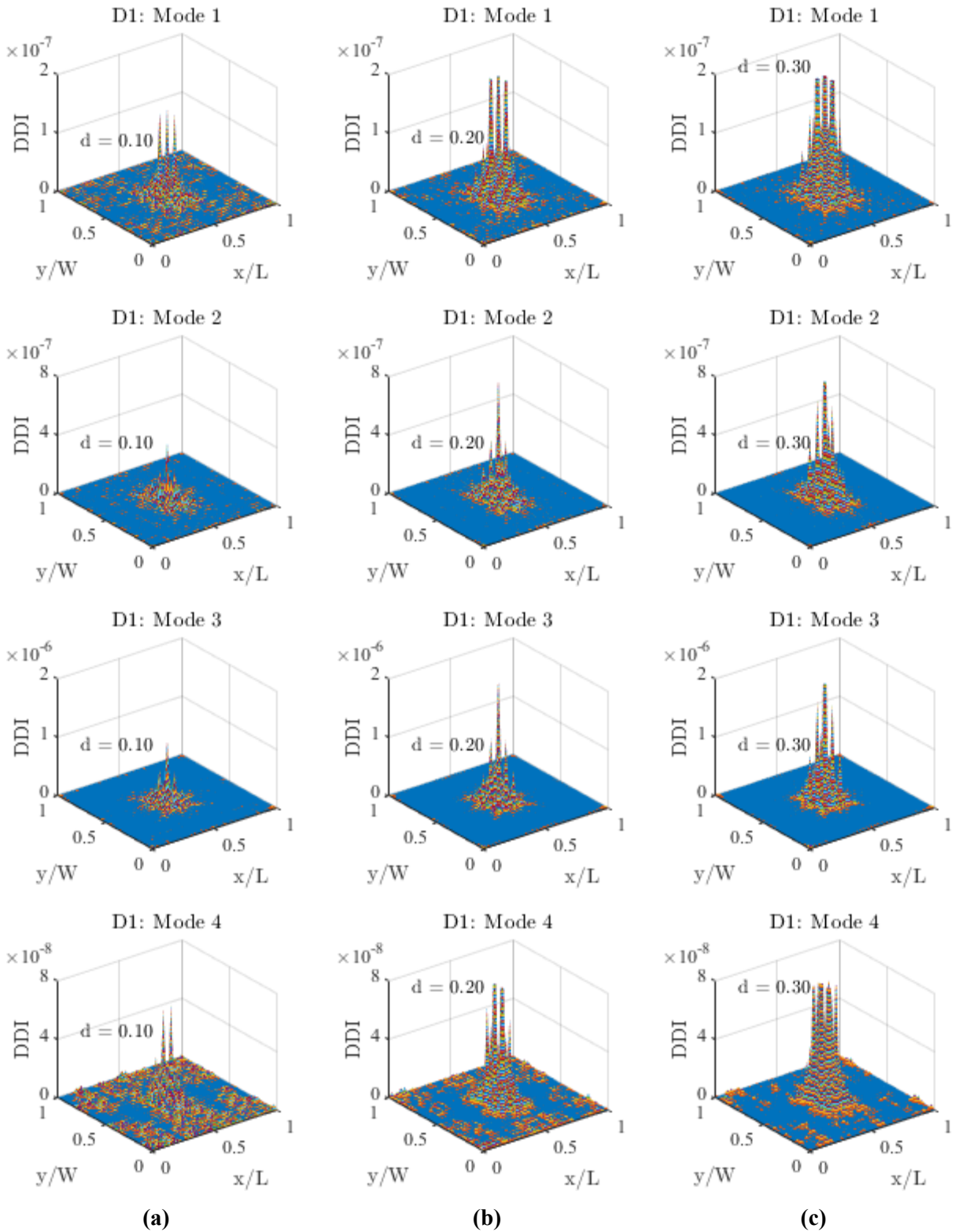
Fig. 4. DDI diagram of the first to 4th modes of the damage scenario D1 with a damage severity of (a) 10%, (b) 20%, and (c) 30%.
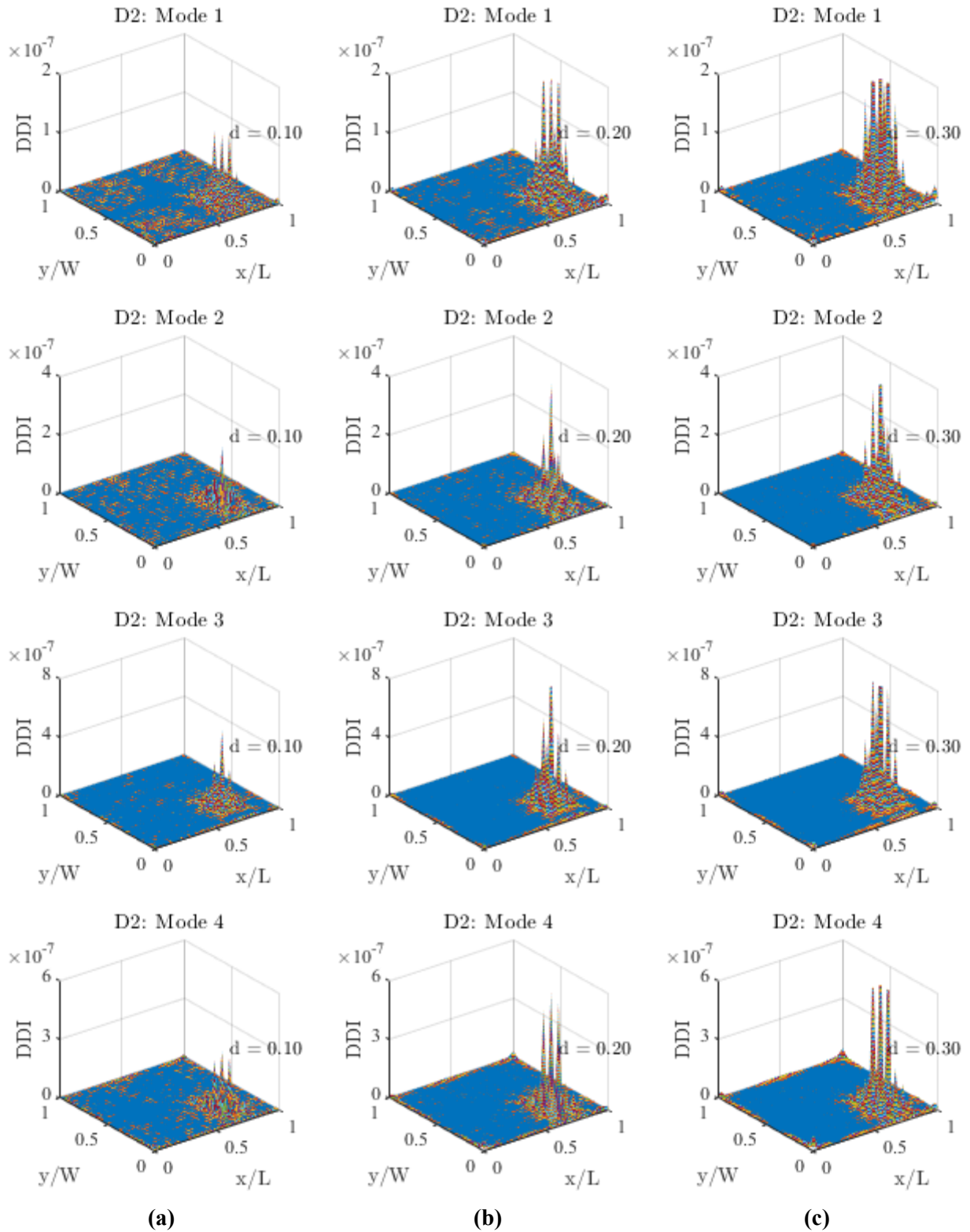
Fig. 5. DDI diagram of the first to 4th modes of the damage scenario D2 with a damage severity of (a) 10%, (b) 20%, and (c) 30%.
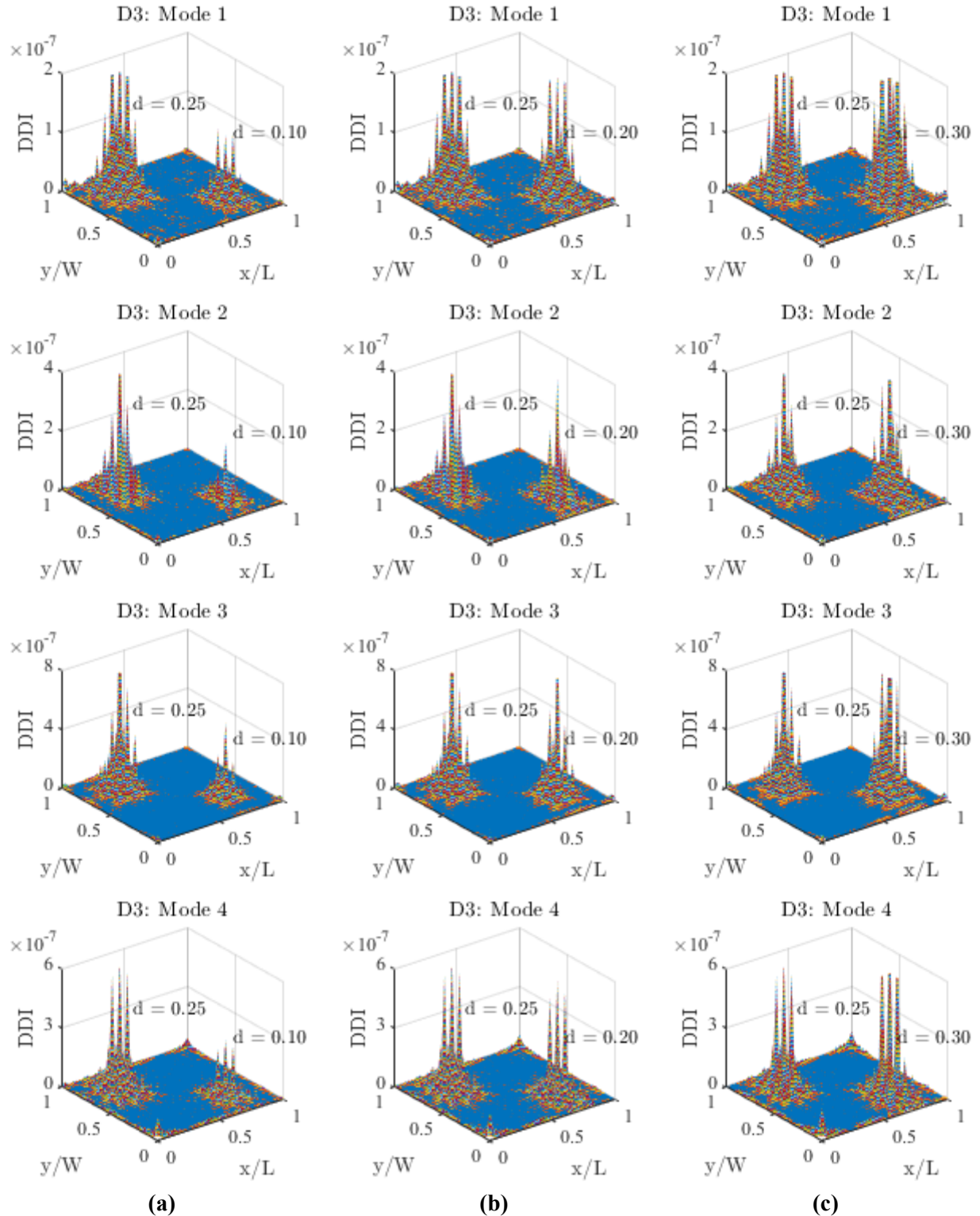
Fig. 6. DDI diagram of the first to 4th modes of the damage scenario D3 with a damage severity of 25% in location 2 and (a) 10%, (b) 20%, and (c) 30% in location 3.

6. Effect of mode rank on identifying damage locations

In order to explore the effect of mode rank on DDI, identifying damage for damage states are introduced in Table 4 for the ten first modes and maximum amounts of DDI were calculated.

Numerical results are reported in Table 5 and the related charts are plotted in Fig 7. It is seen that chart patterns of DDI_{max} in different damage locations is different. Whereas, these patterns are considered in terms of equal curvature property and instantaneous changes of slope.

**Table 4.** Damage location associated with the effect of mode rank on DDI.

Damage			Damage Range (mm)		Damage location		Damage Severity (%)
States	Number	Location	X	y	x/L	y/W	
D1	1	1	375-425	275-325	0.50	0.50	20
D2	1	2	575-625	125-175	0.75	0.25	30
D3	2	2	575-625	125-175	0.75	0.25	30
		3	175-225	425-475	0.25	0.75	20

Table 5. Maximum DDI of different damage location in the first 10 modes ($*10^{-7}$).

Mode	DDI_{max}-D2 ($*10^{-7}$)	DDI_{max}-D3 ($*10^{-7}$)		Difference between columns 2 and 3 (%)
	Location 2	Location 2	Location 3	
1	3.947	3.927	3.190	0.5093
2	6.706	6.688	5.741	0.2691
3	18.20	18.22	13.71	0.1098
4	8.826	8.812	6.498	0.1589
5	7.629	7.612	7.683	0.2233
6	36.22	36.23	28.56	0.0276
7	31.94	32.09	28.55	0.4674
8	20.40	20.35	17.02	0.2457
9	73.35	73.00	56.03	0.4795
10	83.45	82.86	62.67	0.7120
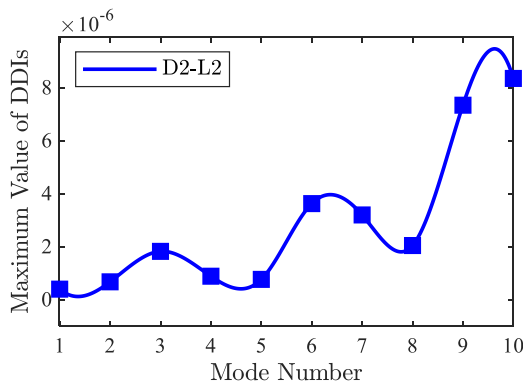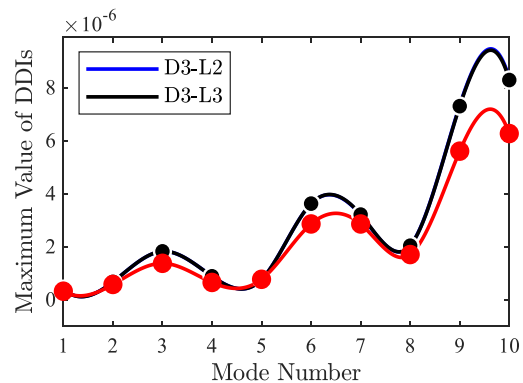
(a) D2   **(b) D3**

Fig. 7. Maximum DDI of damage positions related to the first ten modes of damage location.

Considering Table 5 and charts of Fig. 7, as mentioned, DDI$_{max}$ of different damage locations are different in all modes and in other words they are independent from each other; this subject is clearly shown in Fig. 8. Independency of damage detection index in different damage locations is an advantage in the fields of heath monitoring of structural members; because otherwise, Failure to identifying damage in a location can effect on identifying other damage locations and as a result, some of damage locations would be unidentified. Regarding the results of this topic, proposed index in this article is a successful and practical index in identification of different damage locations.
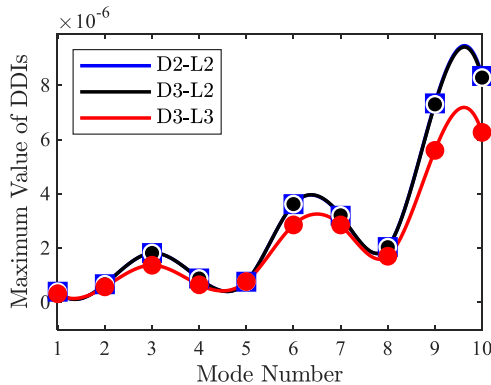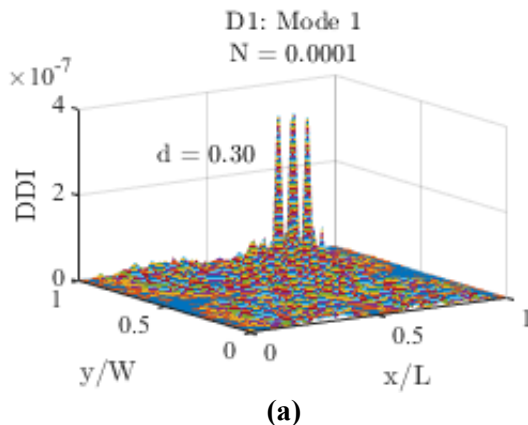

Fig. 8. Maximum DDI of damage positions related to the first ten modes of damage states.

7. Effect of noise on DDI detection index

In laboratory conditions, modal data is affected by random noise. The proposed method for damage detection was investigated by considering the effects of different percentages of noise. The steps of applying the reciprocating effect of random noises to the mode shapes were performed as follows:

Using Equation (19), the r matrix is given random values and the same size as the mode shape signal.

$$r = -1 + 2 * \text{rand}(m, n) \qquad (19)$$

where m and n are the number of rows and columns of the mode shape signal matrix, respectively.

Considering the percentage of noise N and its effect on the mode shape signal using Equation (20),

$$\phi^N = (1 + N. * r). * \phi \qquad (20)$$

where ϕ and ϕ^N are signals in the shape of noiseless and noisy modes, respectively.

Identification of steel plate damage was done for D1 damage state in the first mode with a damage intensity of 30% and noise percentages of 0.01 and 0.025. The damage position has the most disturbance and irregularity, as shown by the graph (Fig. 9).
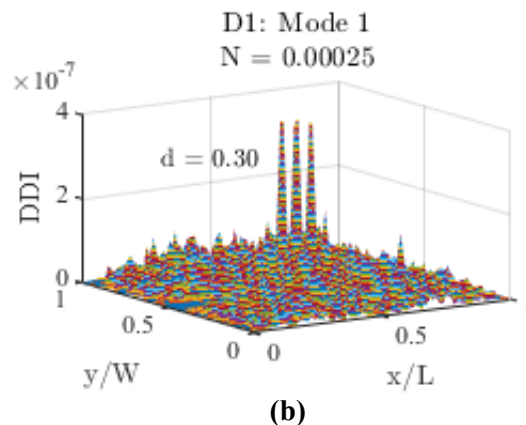

(a)

(b)

Fig. 9. Identification of damage D1 by considering the percentage of noise (a) 0.01% and (b) 0.025%.

8. Conclusion

Structural elements may have minor damage over time, which may be exacerbated by earthquakes, improper excavations, etc. and eventually lead to the collapse of the entire structure at times. Hence, it is vital to pay special attention to structural health monitoring to minimize loss of life and property by repairing or replacing the damaged elements on time. Hence, it is vital to pay special attention to structural health monitoring in order to prevent the occurrence of maximum loss of life and property by repairing or replacing the damaged elements on time. In this study, we addressed the issue of damage detection in steel plates. We found that such damages bring about a difference between the natural frequencies of damaged and undamaged modes. Also, the angle between the shapes of undamaged and their corresponding damaged modes is non-zero; specifically, this angle is always close to zero or 180 degrees. Using the angle between the shape modes, we defined a damage detection index based on the wavelet transform algorithm, which was performed to spot damage locations in the first four modes. The results confirmed the sensitivity of the DDI in different positions; thus, the sensitivity of DDI in fixed spatial coordinates (located in the damaged area) increased with increasing severity of damage. In addition, the results demonstrated that the sensitivity of DDI in each damage location is independent of other similar locations. In other words, changing the severity of a damage in one place leads to a change in the DDI sensitivity of only that location and the DDI of other damage locations is not affected. This finding (independence of DDI sensitivity of damage locations) was obtained by examining the maximum DDI in different damage locations in the first ten modes, and it was observed that DDI_{max} of damage locations follows a fixed and independent pattern as the number of modes rises.

References

[1]   Rytter A. Vibrational based inspection of civil engineering structures. Fract Dyn 1993. https://doi.org/10.1016/j.jsv.2016.06.047.

[2]   Farrar CR, Doebling SW, Nix DA. Vibration–based structural damage identification. Philos Trans R Soc London Ser A Math Phys Eng Sci 2001;359:131–49. https://doi.org/10.1098/rsta.2000.0717.

[3]   Montalvao D. A review of vibration-based structural health monitoring with special emphasis on composite materials. Shock Vib Dig 2006;38:295–324. https://doi.org/10.1177/0583102406065898.

[4]   Chatterjee A. Structural damage assessment in a cantilever beam with a breathing crack using higher order frequency response functions. J Sound Vib 2010;329:3325–34. https://doi.org/10.1016/j.jsv.2010.02.026.

[5]   Majumdar A, Maiti DK, Maity D. Damage assessment of truss structures from changes in natural frequencies using ant colony optimization. Appl Math Comput 2012;218:9759–72. https://doi.org/10.1016/j.amc.2012.03.031.

[6]   Bai RB, Ostachowicz W, Cao MS, Su Z. Crack detection in beams in noisy conditions using scale fractal dimension analysis of mode shapes. Smart Mater Struct 2014;23:065014. https://doi.org/10.1088/0964-1726/23/6/065014.

[7] Yazdanpanah O, Seyedpoor SM, Bengar HA. A new damage detection indicator for beams based on mode shape data. Struct Eng Mech 2015;53:725–44. https://doi.org/10.12989/sem.2015.53.4.725.

[8] Pandey AK, Biswas M, Samman MM. Damage detection from changes in curvature mode shapes. J Sound Vib 1991;145:321–32. https://doi.org/10.1016/0022-460X(91)90595-B.

[9] Tomaszewska A. Influence of statistical errors on damage detection based on structural flexibility and mode shape curvature. Comput Struct 2010;88:154–64. https://doi.org/10.1016/j.compstruc.2009.08.017.

[10] Cao M, Radzieński M, Xu W, Ostachowicz W. Identification of multiple damage in beams based on robust curvature mode shapes. Mech Syst Signal Process 2014;46:468–80. https://doi.org/10.1016/j.ymssp.2014.01.004.

[11] Khanahmadi M, Garfamy HM, Gholhaki M, Rezaifar O, Pouraminian M. Curvature-based damage detection in a column under the effect of axial load. J Struct Steel 2022;16:65–75.

[12] Khanahmadi M, Pouramonian M, Garfamy HM, Dezhkam B. Damage detection and identification in a column under the effect of axial load using modal properties and mode shape-based detection index. Sharif J Civ Eng 2023;38.2:53–62. https://doi.org/10.24200/j30.2022.60873.3129.

[13] Daneshvar MH, Saffarian M, Jahangir H, Sarmadi H. Damage identification of structural systems by modal strain energy and an optimization-based iterative regularization method. Eng Comput 2023;39:2067–87. https://doi.org/10.1007/s00366-021-01567-5.

[14] Hu M, He J, Zhou C, Shu Z, Yang W. Surface damage detection of steel plate with different depths based on Lamb wave. Measurement 2022;187:110364. https://doi.org/10.1016/j.measurement.2021.110364.

[15] Liu X, Lieven NAJ, Escamilla-Ambrosio PJ. Frequency response function shape-based methods for structural damage localisation. Mech Syst Signal Process 2009;23:1243–59. https://doi.org/10.1016/j.ymssp.2008.10.002.

[16] Bandara RP, Chan THT, Thambiratnam DP. Frequency response function based damage identification using principal component analysis and pattern recognition technique. Eng Struct 2014;66:116–28. https://doi.org/10.1016/j.engstruct.2014.01.044.

[17] Bakhary N, Hao H, Deeks AJ. Substructuring technique for damage detection using statistical multi-stage artificial neural network. Adv Struct Eng 2010;13:619–39. https://doi.org/10.1260/1369-4332.13.4.619.

[18] Shu J, Zhang Z, Gonzalez I, Karoumi R. The application of a damage detection method using Artificial Neural Network and train-induced vibrations on a simplified railway bridge model. Eng Struct 2013;52:408–21. https://doi.org/10.1016/j.engstruct.2013.02.031.

[19] He R-S, Hwang S-F. Damage detection by a hybrid real-parameter genetic algorithm under the assistance of grey relation analysis. Eng Appl Artif Intell 2007;20:980–92. https://doi.org/10.1016/j.engappai.2006.11.020.

[20] Meruane V, Heylen W. Structural damage assessment with antiresonances versus mode shapes using parallel genetic algorithms. Struct Control Heal Monit

2011;18:825–39. https://doi.org/10.1002/stc.401.

[21] Chandrashekhar M, Ganguli R. Damage assessment of structures with uncertainty by using mode-shape curvatures and fuzzy logic. J Sound Vib 2009;326:939–57. https://doi.org/10.1016/j.jsv.2009.05.030.

[22] Nguyen SD, Ngo KN, Tran QT, Choi SB. A new method for beam-damage-diagnosis using adaptive fuzzy neural structure and wavelet analysis. Mech Syst Signal Process 2013;39:181–94. https://doi.org/10.1016/j.ymssp.2013.03.02 3.

[23] Reda Taha MM, Noureldin A, Lucero JL, Baca TJ. Wavelet transform for structural health monitoring: A compendium of uses and features. Struct Heal Monit 2006;5:267–95. https://doi.org/10.1177/147592170606774 1.

[24] Andreaus U, Baragatti P, Casini P, Iacoviello D. Experimental damage evaluation of open and fatigue cracks of multi-cracked beams by using wavelet transform of static response via image analysis. Struct Control Heal Monit 2017;24. https://doi.org/10.1002/stc.1902.

[25] Zhou S, Tang B, Chen R. Comparison between non-stationary signals fast Fourier transform and wavelet analysis. Int Asia Symp Intell Interact Affect Comput ASIA 2009 2009:128–9. https://doi.org/10.1109/ASIA.2009.31.

[26] Newland DE. Wavelet Analysis of Vibration, Part 1: Theory; Part 2: Wavelet Maps. J Vib Acoust 1994;116:409–25.

[27] Masuda, A., Nakaoka, A., Sone, A., and Yamamoto S. Health monitoring system of structures based on orthonormal wavelet transform. Seism Engrg 1995;312:161–7.

[28] Wang Q, Deng X. Damage detection with spatial wavelets. Int J Solids Struct 1999;36:3443–68. https://doi.org/10.1016/S0020-7683(98)00152-8.

[29] Hou Z, Hera A, Noori M. Wavelet-based techniques for structural health monitoring. Heal Assess Eng Struct Bridg Build Other Infrastructures 2013:179–202. https://doi.org/10.1142/9789814439022_0 007.

[30] Douka E, Loutridis S, Trochidis A. Crack identification in plates using wavelet analysis. J Sound Vib 2004;270:279–95. https://doi.org/10.1016/S0022-460X(03)00536-4.

[31] Ovanesova A V., Suárez LE. Applications of wavelet transforms to damage detection in frame structures. Eng Struct 2004;26:39–49. https://doi.org/10.1016/j.engstruct.2003.08. 009.

[32] Loutridis S, Douka E, Trochidis A. Crack identification in double-cracked beams using wavelet analysis. J Sound Vib 2004;277:1025–39. https://doi.org/10.1016/j.jsv.2003.09.035.

[33] Chang CC, Chen LW. Detection of the location and size of cracks in the multiple cracked beam by spatial wavelet based approach. Mech Syst Signal Process 2005;19:139–55. https://doi.org/10.1016/j.ymssp.2003.11.00 1.

[34] Khatam H, Golafshani AA, Beheshti-Aval SB, Noori M. Harmonic class loading for damage identification in beams using wavelet analysis. Struct Heal Monit 2007;6:67–80. https://doi.org/10.1177/147592170707206 4.

[35] Fan W, Qiao P. A 2-D continuous wavelet transform of mode shape data for damage detection of plate structures. Int J Solids Struct 2009;46:4379–95. https://doi.org/10.1016/j.ijsolstr.2009.08.0 22.

[36] Gökdağ H, Kopmaz O. A new damage detection approach for beam-type structures based on the combination of continuous and discrete wavelet

transforms. J Sound Vib 2009;324:1158–80. https://doi.org/10.1016/j.jsv.2009.02.030.

[37] Katunin A. Identification of multiple cracks in composite beams using 2010:41–52.

[38] Zhong S, Oyadiji SO. Crack detection in simply supported beams using stationary wavelet transform of modal data. Struct Control Heal Monit 2011;18:169–90. https://doi.org/10.1002/stc.366.

[39] Bagheri A, Kourehli S. Damage detection of structures under earthquake excitation using discrete wavelet analysis. Asian J Civ Eng 2013;14:289–304.

[40] Xu W, Radzieński M, Ostachowicz W, Cao M. Damage detection in plates using two-dimensional directional Gaussian wavelets and laser scanned operating deflection shapes. Struct Heal Monit 2013;12:457–68. https://doi.org/10.1177/147592171349236 5.

[41] Lee SG, Yun GJ, Shang S. Reference-free damage detection for truss bridge structures by continuous relative wavelet entropy method. Struct Heal Monit 2014;13:307–20. https://doi.org/10.1177/147592171452284 5.

[42] Li J, Hao H. Substructure damage identification based on wavelet-domain response reconstruction. Struct Heal Monit 2014;13:389–405. https://doi.org/10.1177/147592171453299 1.

[43] Katunin A. Stone impact damage identification in composite plates using modal data and quincunx wavelet analysis. Arch Civ Mech Eng 2015;15:251–61. https://doi.org/10.1016/j.acme.2014.01.010 .

[44] Patel SS, Chourasia AP, Panigrahi SK, Parashar J, Parvez N, Kumar M. Damage Identification of RC Structures Using Wavelet Transformation. Procedia Eng

2016;144:336–42. https://doi.org/10.1016/j.proeng.2016.05.1 41.

[45] Asgarian B, Aghaeidoost V, Shokrgozar HR. Damage detection of jacket type offshore platforms using rate of signal energy using wavelet packet transform. Mar Struct 2016;45:1–21. https://doi.org/10.1016/j.marstruc.2015.10. 003.

[46] Ashory MR, Ghasemi-Ghalebahman A, Kokabi MJ. Damage identification in composite laminates using a hybrid method with wavelet transform and finite element model updating. Proc Inst Mech Eng Part C J Mech Eng Sci 2018;232:815–27. https://doi.org/10.1177/095440621769284 4.

[47] Yang C, Oyadiji SO. Delamination detection in composite laminate plates using 2D wavelet analysis of modal frequency surface. Comput Struct 2017;179:109–26. https://doi.org/10.1016/j.compstruc.2016.1 0.019.

[48] Zhao Y, Noori M, Altabey WA, Beheshti-Aval SB. Mode shape-based damage identification for a reinforced concrete beam using wavelet coefficient differences and multiresolution analysis. Struct Control Heal Monit 2018;25. https://doi.org/10.1002/stc.2041.

[49] Younesi A, Rezaifar O, Gholhaki M, Esfandiari A. Structural health monitoring of a concrete-filled tube column. Mag Civ Eng 2019;85:136–45. https://doi.org/10.18720/MCE.85.11.

[50] Younesi A, Rezaifar O, Gholhaki M, Esfandiari A. Damage detection in concrete filled tube columns based on experimental modal data and wavelet technique. Mech Adv Compos Struct 2020;7:245–54. https://doi.org/10.22075/macs.2020.17087. 1195.

[51] Younesi A, Rezaifar O, Gholhaki M, Esfandiari A. Active interface debonding detection of a concrete filled tube (CFT) column by modal parameters and continuous wavelet transform (CWT) technique. Struct Monit Maint 2021;8:69–90. https://doi.org/10.12989/smm.2021.8.1.069.

[52] Wang S, Li J, Luo H, Zhu H. Damage identification in underground tunnel structures with wavelet based residual force vector. Eng Struct 2019;178:506–20. https://doi.org/10.1016/j.engstruct.2018.10.021.

[53] Khanahmadi M, Rezaifar O, Gholhaki M. Damage detection in steel plates based on comparing analytical results of the discrete 2-D wavelet transform of primary and secondary modes shape. J Struct Constr Eng 2021;8:198–214. https://doi.org/10.22065/jsce.2019.174347.1799.

[54] Khanahmadi M, Rezaifar O, Gholhaki M. Damage detection of prefabricated walls (panel 3D plates) based on wavelet transform detection algorithm. J Struct Constr Eng 2021;8:289–309. https://doi.org/10.22065/jsce.2019.197470.1923.

[55] Khanahmadi M, Gholhaki M, Ghasemi-Ghalebahman A, Khademi-Kouhi M. Damage detection in laminated composite plates using wavelet analysis analytical method. J Vib Sound 2022;10:144–56.

[56] Khanahmadi M, Gholhaki M, Rezaifar O. Damage identification of a column under the axial load based on wavelet transform and modal data. J Model Eng 2021;18:51–64. https://doi.org/10.22075/JME.2020.20940.1931.

[57] Khanahmadi M, Garfamy HM, Gholhaki M, Dezhkam B, Miri ME. Wavelet-based damage detection of steel beam-structures. J Struct Steel 2021;15:15–27.

[58] Khanahmadi M, Rezaifar O, Gholhaki M. Comparative study on steel beams damage detection based on continuous and discrete wavelet transforms of static and dynamic responses. J Struct Constr Eng 2021;8:166–83. https://doi.org/10.22065/JSCE.2020.216647.2058.

[59] Khanahmadi M, Rezaifar O, Gholhaki M, Dezhkam B, Younesi A. Health monitoring and damage assessment of a column under the effect of axial load using modal dynamic data and wavelet analytical method. Modares Civ Eng J 2023;23:7–25. https://doi.org/10.22034/23.3.7.

[60] Rezaifar O, Gholhaki M, Khanahmadi M, Amiri Y. A review of structural health monitoring and damage detection using wavelet transform: the case study of damage detection in cantilever beams. J Vib Sound 2022;11:157–71.

[61] Jahangir H, Khatibinia M, Mokhtari Masi M. Damage detection in prestressed concrete slabs using wavelet analysis of vibration responses in the time domain. J Rehabil Civ Eng 2022;10:37–63. https://doi.org/10.22075/jrce.2021.23385.1510.

[62] Jahangir H, Hasani H, Esfahani MR. Damage localization of RC beams via wavelet analysis of noise contaminated modal curvatures. J Soft Comput Civ Eng 2021;5:101–33. https://doi.org/10.22115/SCCE.2021.292279.1340.

[63] Mamazizi A, Khanahmadi M, Nobakht Vakili K. Debonding damage detection and assessment in a CFST composite column using modal dynamic data. Sharif J Civ Eng 2022;38.2:53–63. https://doi.org/10.24200/j30.2022.59903.3075.

[64] Khanahmadi M, Rezaifar O, Gholhaki M, Younesi A. Detection of debonding damage location of the concrete core from the steel tube of concrete-filled steel tube (CFST) columns using wavelet analysis

analytical method. Modares Civ Eng J 2023;22:129–42.

[65]   Khanahmadi M, Gholhaki M, Rezaifar O, Dezhkam B. Damage identification in steel beam structures based on the comparison of analytical results of wavelet analysis. Civ Infrastruct Res 2023;8:173–83. https://doi.org/10.22091/cer.2022.8340.14 07.

[66]   Benedetto JJ, Walnut DF. Gabor frames for L2 and related spaces. Wavelets 2021:97–162. https://doi.org/10.1201/9781003210450-4.

[67]   Rao KR, Kim DN, Hwang J-J. Fast Fourier Transform - Algorithms and Applications 2010:340.

[68]   Douka E, Loutridis S, Trochidis A. Crack identification in beams using wavelet analysis. Int J Solids Struct 2003;40:3557–69. https://doi.org/10.1016/S0020-7683(03)00147-1.

[69]   Zhong S, Oyadiji SO. Detection of cracks in simply-supported beams by continuous wavelet transform of reconstructed modal data. Comput Struct 2011;89:127–48. https://doi.org/10.1016/j.compstruc.2010.0 8.008.

[70]   Kim H, Melhem H. Damage detection of structures by wavelet analysis. Eng Struct 2004;26:347–62. https://doi.org/10.1016/j.engstruct.2003.10. 008.

[71]   Abdulkareem M, Bakhary N, Vafaei M, Noor NM, Padil KH. Non-probabilistic wavelet method to consider uncertainties in structural damage detection. J Sound Vib 2018;433:77–98. https://doi.org/10.1016/j.jsv.2018.07.011.

[72]   Hoseini Vaez SR, Dehghani E, Babaei V. Damage Detection in Post-tensioned Slab Using 2D Wavelet Transforms. J Rehabil Civ Eng 2017;5:25–38. https://doi.org/10.22075/JRCE.2017.11561 .1191.

[73]   Rezaifar O, Kabir MZ, Taribakhsh M, Tehranian A. Dynamic behaviour of 3D-panel single-storey system using shaking table testing. Eng Struct 2008;30:318–37. https://doi.org/10.1016/j.engstruct.2007.03. 019.

[74]   Kabir MZ, Rezaifar O. Shaking table examination on dynamic characteristics of a scaled down 4-story building constructed with 3D-panel system. Structures 2019;20:411–24. https://doi.org/10.1016/j.istruc.2019.05.00 6.

[75]   Naderpour H, Fakharian P. A synthesis of peak picking method and wavelet packet transform for structural modal identification. KSCE J Civ Eng 2016;20:2859–67. https://doi.org/10.1007/s12205-016-0523-4.

[76]   Fakharian P, Naderpour H. Damage Severity Quantification Using Wavelet Packet Transform and Peak Picking Method. Pract Period Struct Des Constr 2022;27:1–11. https://doi.org/10.1061/(asce)sc.1943-5576.0000639.